

Annex E

Drill Cuttings and Muds Dispersion Modelling

Tamarind - Tui Field

Drill Cuttings and Muds Dispersion Modelling

Prepared by:	RPS AUSTRALIA WEST PTY LTD Suite E1, Level 4 140 Bundall Road Bundall, QLD 4217 Australia	Prepared for:	ERM NEW ZEALAND 117 Powderham St New Plymouth 4310 New Zealand
T:	+61 7 5574 1112	T:	+64 (0)9 3034 664
E:	Nathan.Benfer@rpsgroup.com.au	E:	Alison.Lane@erm.com
		W:	erm.com.au
Author:	Nathan Benfer		
Reviewed:	Sasha Zigic		
Approved:	Nathan Benfer		
No.:	MAQ0648J		
Version:	2		
Date:	21/03/2018		

Document Status

Version	Purpose of Document	Approved by	Reviewed by	Review Date
0	Draft Issued to Client	Nathan Benfer	Sasha Zigic	31/01/2018
1	Issued to Client	Nathan Benfer	Sasha Zigic	12/02/2018
2	Issued to Client	Nathan Benfer	Sasha Zigic	21/03/2018

Approval for issue

Name	Signature	Date
Nathan Benfer		21/03/2018

This report was prepared by [RPS Australia West Pty Ltd ('RPS')] within the terms of its engagement and in direct response to a scope of services. This report is strictly limited to the purpose and the facts and matters stated in it and does not apply directly or indirectly and must not be used for any other application, purpose, use or matter. In preparing the report, RPS may have relied upon information provided to it at the time by other parties. RPS accepts no responsibility as to the accuracy or completeness of information provided by those parties at the time of preparing the report. The report does not take into account any changes in information that may have occurred since the publication of the report. If the information relied upon is subsequently determined to be false, inaccurate or incomplete then it is possible that the observations and conclusions expressed in the report may have changed. RPS does not warrant the contents of this report and shall not assume any responsibility or liability for loss whatsoever to any third party caused by, related to or arising out of any use or reliance on the report howsoever. No part of this report, its attachments or appendices may be reproduced by any process without the written consent of RPS. All enquiries should be directed to RPS.

Contents

EXECUTIVE SUMMARY	6
1 INTRODUCTION	8
1.1 Project Background	8
2 SCOPE OF WORK	10
3 REGIONAL CURRENTS	10
3.1 Tidal Currents	12
3.1.1 Grid Setup	12
3.1.2 Tidal Conditions	14
3.1.3 Surface Elevation Validation	14
3.2 Ocean Currents	19
3.3 Currents at the Release Site	20
4 WATER TEMPERATURE AND SALINITY	22
5 SEDIMENT DISPERSION MODELLING	24
5.1 Model Description - MUDMAP	24
5.2 Discharge Program	25
5.3 Discharge Input Data	26
5.4 Grid Configuration	29
5.5 Mixing Parameters	29
5.6 Minimum Reporting Thresholds	29
6 RESULTS	30
7 REFERENCES	36

Tables

Table 1	Coordinates of the release sites used in the study.	8
Table 2	Statistical comparison between the observed and HYDROMAP predicted surface elevations data from the 1 st to 31 st January 2014.	15
Table 3	Predicted average and maximum surface current speeds at the study site. The data was derived by combining the HYCOM ocean data and HYDROMAP tidal data for 2008-2012 (inclusive).	20
Table 4	Monthly average sea-surface temperature and salinity at the study area.	22
Table 5	Summary of the estimated volume of discharged drill cuttings and unrecoverable mud solids for each well.	26
Table 6	Input data used for the drill cuttings and unrecoverable mud solids dispersion modelling.	27
Table 7	Discharged grain size distribution and settling velocities assumed for the production wells consisting of cuttings and water-based mud.	28
Table 8	Predicted bottom deposition, area of coverage and maximum distance to the minimum threshold for each well.	31
Table 9	Total area covered for each bottom deposition range for Amokura-2H.	31
Table 10	Total area covered for each bottom deposition range for Tui-2H and 3H combined.	31
Table 11	Total area covered for each bottom deposition range for Pateke-3H.	31
Table 12	Predicted total suspended solids concentration for each well.	32
Table 13	Total area covered for each total suspended solids concentration range for Amokura-2H.	32
Table 14	Total area covered for each total suspended solids concentration range for Tui-2H and 3H combined.	32
Table 15	Total area covered for each total suspended solids concentration range for Pateke-3H.	32

Figures

Figure 1	Location of the release sites used in the modelling study.	9
Figure 2	Schematic showing the oceanic current circulation surrounding New Zealand (Image source: Brodie, 1960).....	11
Figure 3	Map showing the regions of sub-gridding for the study area	13
Figure 4	Bathymetry used in the hydrodynamic grid for the study region.....	13
Figure 5	Location of the nine tide stations around New Zealand used to validate the tidal model.	15
Figure 6	Comparison between predicted (red line) and observed (blue line) surface elevation variation at Auckland (top), Bluff (middle) and Lyttelton (bottom), between the 1 st and the 31 st of January 2014.	16
Figure 7	Comparison between predicted (red line) and observed (blue line) surface elevation variation at Napier (top), Nelson (middle) and Picton (bottom), between the 1 st and the 31 st of January 2014.	17
Figure 8	Comparison between predicted (red line) and observed (blue line) surface elevation variation at Port Taranaki (top), Wellington (middle) and Westport (bottom), between the 1 st and 31 st of January 2014.....	18
Figure 9	Snapshot example of the predicted HYCOM ocean surface currents in the region. Colour of individual arrows indicate current speed (m/s).....	19
Figure 10	Predicted monthly surface current rose plots at the study site. Data was derived by combining the HYDROMAP tidal currents and HYCOM ocean currents for 2008 – 2012. The colour key shows the current speed (m/s), the compass direction provides the current direction flowing TOWARDS and the length of the wedge gives the percentage of the record for a particular speed and direction combination.	21
Figure 11	Monthly average sea temperature and salinity profiles at the study site.	23
Figure 12	Conceptual diagram showing the general behaviour of cuttings and muds following discharge to the ocean (Neff, 2005) and the idealised representation of the three discharge phases.	25
Figure 13	Predicted bottom deposition and coverage from drill cuttings and unrecoverable mud solids on the seafloor for Amokura-2H.	33
Figure 14	Predicted bottom deposition and coverage from drill cuttings and unrecoverable mud solids on the seafloor for Tui-2H and 3H combined.	33
Figure 15	Predicted bottom deposition and coverage from drill cuttings and unrecoverable mud solids on the seafloor for Pateke-3H.	34
Figure 16	Predicted peak total suspended solids from drill cuttings and unrecoverable mud solids in the water column for Amokura-2H.	34
Figure 17	Predicted peak total suspended solids from drill cuttings and unrecoverable mud solids in the water column for Tui-2H and 3H combined.	35
Figure 18	Predicted peak total suspended solids from drill cuttings and unrecoverable mud solids in the water column for Pateke-3H.....	35

Executive Summary

Project Background

Tamarind Resources (Tamarind) is planning to undertake side-track drilling activities for 4 wells in the Tui field in the Taranaki Basin, about 46 km off the Taranaki coastline in approximately 122 meters of water.

Tamarind has indicated that the wells will reuse existing conductor holes, so these new sections will consist of only 8½" production holes. Drilling will commence first at Amokura-2H, then Tui-2H and 3H, followed by Pateke-3H and drilling durations for each well varied from 11.8 days to 17.8 days. All sections will be using water-based muds. A riser would be fitted to circulate cuttings and drilling fluid to the drilling rig where the cuttings and muds would be separated before the cuttings and unrecoverable mud solids are discharged at a depth of 10 m below the sea surface from a vertically downward orientated discharge pipe. Estimates for the volumes of mud solids discharged during this drilling are based on assumed rates of loss from the separation system, adhering to the cuttings.

To support development of the Environmental Plan for the project, RPS was commissioned to carry out a sediment dispersion modelling study to provide guidance on the seabed deposition and in-water total suspended solids concentrations (TSS) from the cuttings and drilling muds discharge.

Methodology

The modelling study was carried out in several stages. Firstly, samples of three-dimensional (3D) current data for the Taranaki Basin were generated to represent the combined influence of ocean drift currents and tidal currents. Secondly, the current data and discharge characteristics were input into a sediment dispersion model, MUDMAP, to predict the movement and initial settlement of cuttings and drilling mud particles based on an expected sediment grain size distribution for the mixtures.

The threshold adopted for sea floor deposition was calculated using a conservatively assumed background sedimentation rate of 10 g/m²/day. This sedimentation rate, multiplied by 40 days, which is the average time to complete each well, provides a deposition threshold of 400 g/m². This deposition threshold was converted to a minimum thickness by considering the average bulk density of the cuttings and mud solids. To account for voids within the newly settled cuttings and muds a bulking factor of 2.5 was applied to give a final minimum deposition thickness threshold of 0.4 mm (or 400 µm). This same bulking factor was applied to the modelling results.

Total suspended solids (TSS) thresholds were set to a conservative level of 1 mg/l.

Results

Maximum thickness on the sea floor ranged from 86 mm for the Pateke-3H well to 105 mm for the combined Tui wells. These maximum thicknesses occurred within 20 meters of the well.

Sea floor deposition greater than the 0.4 mm threshold reached maximum distances ranging from 204m for the Amokura-2H well to 306m for the combined Tui wells.

The maximum areas of sea floor coverage above the minimum threshold of 0.4 mm ranged from 84,930 m² (0.085 km²) for the Amokura-2H well to 194,600 m² (0.195 km²) for the combined Tui wells.

Peak TSS values at the well sites were consistent, with a maximum of 33 mg/l.



Maximum peak TSS values greater than the 1 mg/l threshold reached maximum distances ranging from 500 m for the Amokura-2H well to 571 m for the Pateke-3H well.

The total areas of influence by TSS values greater than the threshold of 1 mg/l ranged from 282,390 m² (0.282 km²) for the Amokura-2H well to 604,000 m² (0.604 km²) for the combined Tui wells.

TSS concentrations of 10 mg/l were only observed in the top 20 m of the water column, while TSS concentrations down to 2 mg/l were only observed down to 30 or 40 m.

TSS concentrations greater than 1 mg/l extended almost all the way to the seabed directly under the discharge site, due to material falling through this column of water, however further afield TSS concentrations greater than 1 mg/l were only observed in the top 30 to 40 m of the water column.

1 Introduction

1.1 Project Background

Tamarind Resources (Tamarind) is planning to undertake side-track drilling activities for 4 wells in the Tui field (Table 1) in the Taranaki Basin, about 46 km off the Taranaki coastline in approximately 122 meters depth of water (Table 1 and Figure 1).

Tamarind has indicated that the wells will reuse existing conductor holes, so these new sections will consist of only 8½" production holes. Drilling will commence first at Amokura-2H, then Tui-2H and 3H, followed by Pateke-3H and drilling durations for each well varied from 11.8 days to 17.8 days. All sections will be using water-based muds and a riser would be fitted to circulate cuttings and drilling fluid to the drilling rig where the cuttings and muds would be separated before the cuttings and unrecoverable mud solids are discharged at a depth of 10 m below the sea surface from a vertically downward orientated discharge pipe. Estimates for the volumes of mud solids discharged during this drilling are based on assumed rates of loss from the separation system, adhering to the cuttings.

To support development of the Environmental Plan for the project, RPS was commissioned to carry out a sediment dispersion modelling study to provide guidance on the seabed deposition and in-water total suspended solids concentrations from the cuttings and drilling muds discharge.

Table 1 Coordinates of the release sites used in the study.

Well name	Latitude	Longitude	Water depth (m)
Amokura-2H ST1	39° 25' 23" S	173° 12' 44" E	123
Tui-2H ST1	39° 26' 35" S	173° 14' 11" E	122
Tui-3H ST1	39° 26' 34" S	173° 14' 9" E	122
Pateke-3H ST2	39° 22' 52" S	173° 12' 25" E	123

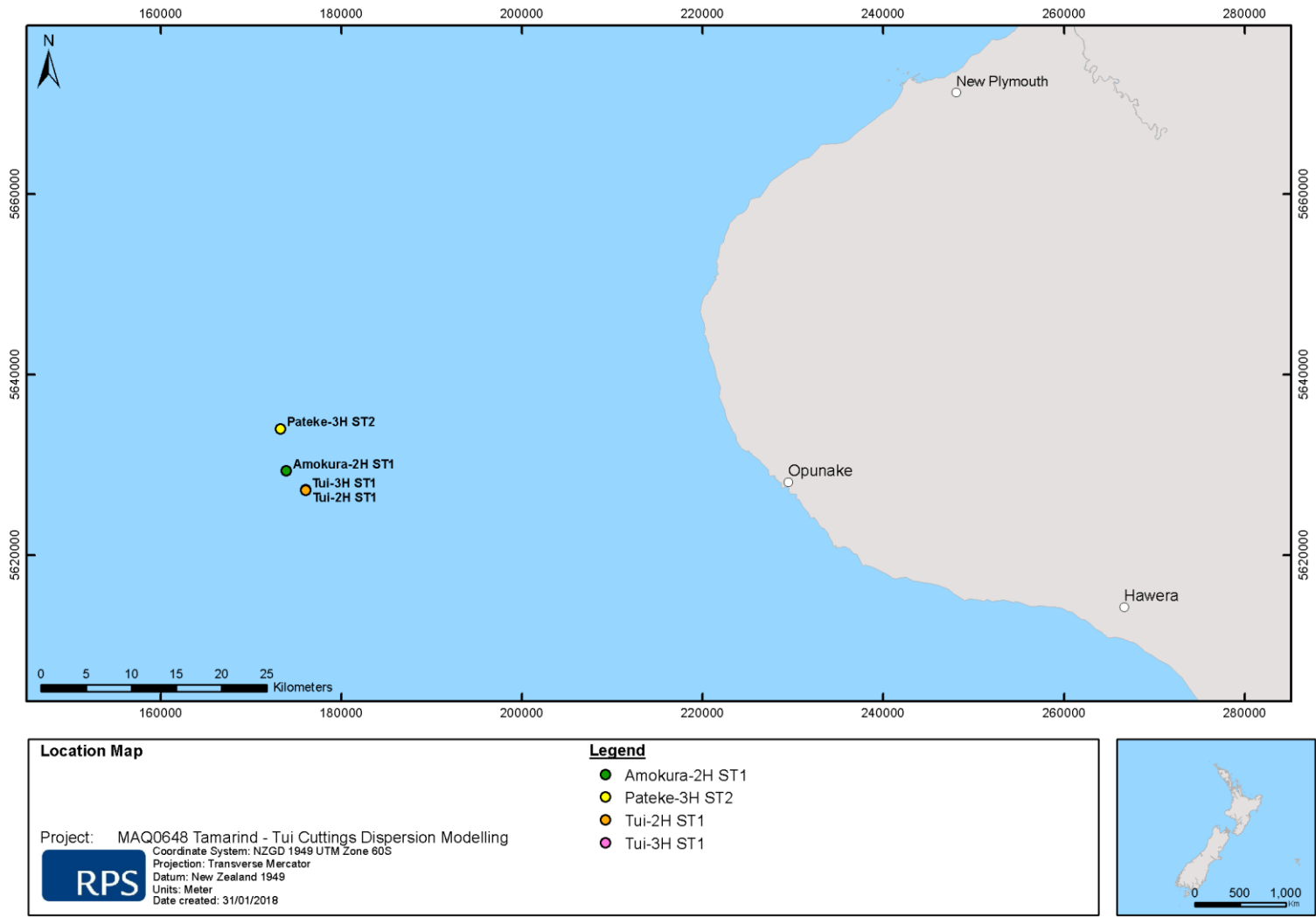


Figure 1 Location of the release sites used in the modelling study.

2 Scope of Work

The scope of work included the following components:

- Generate three-dimensional (3D) currents for the study area that includes the combined influence of ocean and tidal currents for 2012;
- Summarise the drilling plans and discharge characteristics as input into the sediment dispersion model, MUDMAP;
- Simulate all stages of the drilling programme; and
- Analyse and process the MUDMAP results to map the distribution and thicknesses of discharged cuttings and muds on the sea floor and concentrations of total suspended solids (TSS) in the upper water column.

3 Regional Currents

An extensive review of the ocean circulation surrounding New Zealand, which describes the ocean currents in the region, is provided by Heath (1985). The study describes two main surface water masses which surround New Zealand, which include the Subtropical and Subantarctic Surface waters. The Subtropical waters predominately originate from an extension of the East Australian Current (EAC), which is a western boundary current that flows from the South Equatorial Current (SEC), and down the eastern coast of Australia. Typically, the EAC carries warm waters to the south, before splitting off into the Tasman Sea approximately in line with Sydney (Coleman, 1984) and carrying the warmer waters eastwards towards New Zealand (Heath, 1985). The Subantarctic Water tends to flow northwards along the eastern side of the South Island, originating from the Circumpolar Current south of New Zealand.

Figure 2 presents a schematic of the regional currents of New Zealand.

The oceanic currents near the Taranaki Basin are predominately influenced by the typically eastward flowing D'Urville Current and the northward flowing Westland Current. The D'Urville Current consists of warm saline water that flows eastwards into the Cook Strait from the west-northwest (Brodie, 1960; Heath, 1985). The Westland Current has been observed to flow predominately northwards along the west coast of the South Island, where it then mixes with the D'Urville near the Cook Strait. An extension of the Westland current has been observed to extend further northwards along the western coast of the North Island. Previous work by Bowman et al. (1983) indicate that strong non-tidal flows through the Cook Strait may be influenced strongly by the prevailing winds, as shown by a pair of drifters which were observed to travel from the Taranaki Bight through the Cook Strait in a south easterly direction, with strong prevailing winds from the northwest.

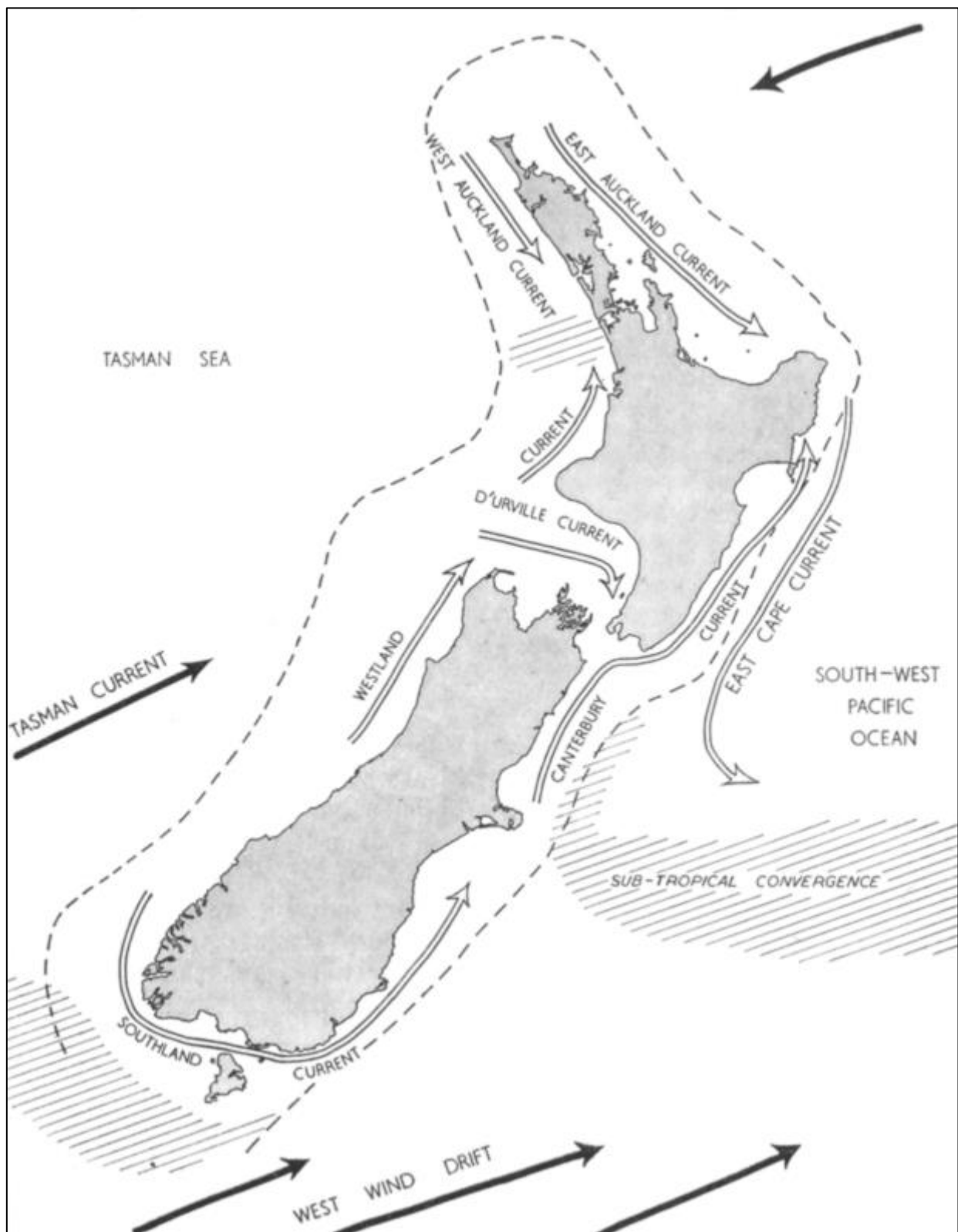


Figure 2 Schematic showing the oceanic current circulation surrounding New Zealand (Image source: Brodie, 1960).

3.1 Tidal Currents

The effects of tides were generated using RPS's advanced ocean/coastal model, HYDROMAP. The HYDROMAP model has been thoroughly tested and verified through field measurements throughout the world over more than 20 years (Isaji and Spaulding, 1984; Isaji et al., 2001; Zigic et al., 2003). In fact, HYDROMAP tidal current data has been used as input for the OILMAP hydrocarbon spill modelling system, which forms part of the Incident Management System (IMS) operated by Maritime New Zealand (MNZ).

HYDROMAP employs a sophisticated sub-gridding strategy, which supports up to six levels of spatial resolution, halving the grid cell size as each level of resolution is employed. The sub-gridding allows for higher resolution of currents within areas of greater bathymetric and coastline complexity, and/or of particular interest to a study.

The numerical solution methodology follows that of Davies (1977a and 1977b) with further developments for model efficiency by Owen (1980) and Gordon (1982). A more detailed presentation of the model can be found in Isaji and Spaulding (1984) and Isaji et al. (2001).

3.1.1 Grid Setup

HYDROMAP was set-up to cover the domain of interest, which was subdivided horizontally into a grid with 4 levels of resolution. The resolution of the primary level was set at 8 km. The resolution of the first, second and third levels were 4 km, 2 km, 1 km respectively. The finer grids were allocated in a step-wise fashion to more accurately resolve flows along the coastline, around islands and over more complex bathymetry. Figure 3 shows a zoomed in image in the region containing the Pateke-4H release site.

A combination of datasets was used to describe the shape of the seabed within the high-resolution grid. Depths for the region were extracted from nautical charts and the SRTM30_PLUS dataset (see Becker et al., 2009), which provides a 30-arc second, or approximately 1 km, resolution (see Figure 4).

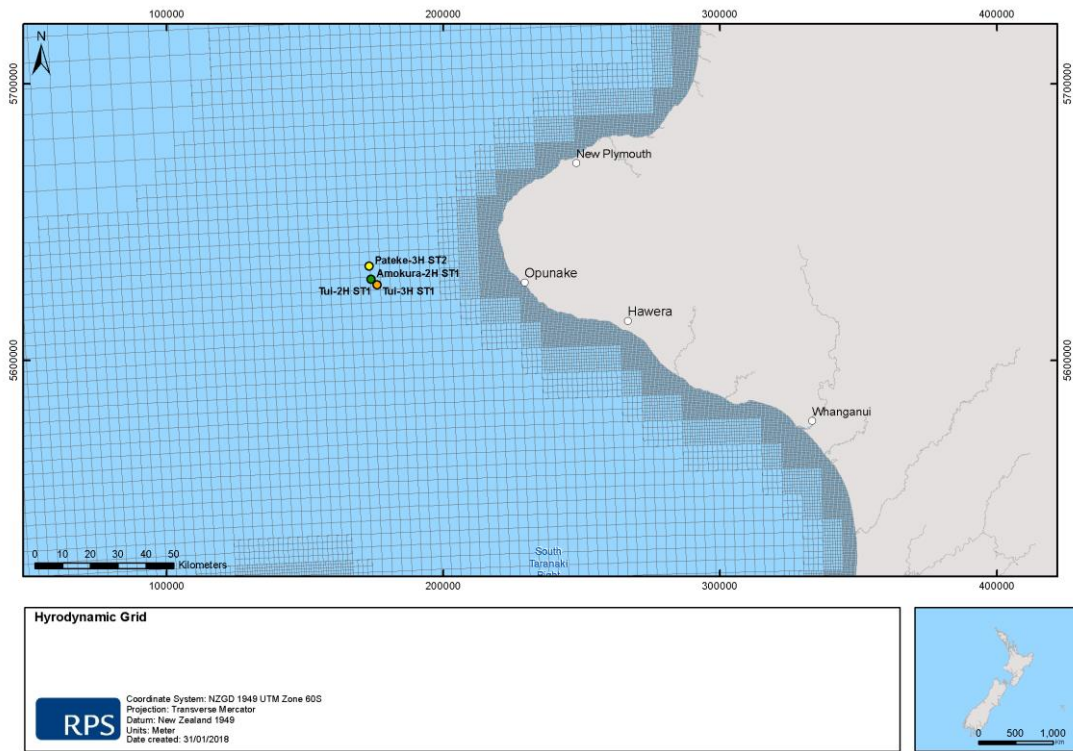


Figure 3 Map showing the regions of sub-gridding for the study area

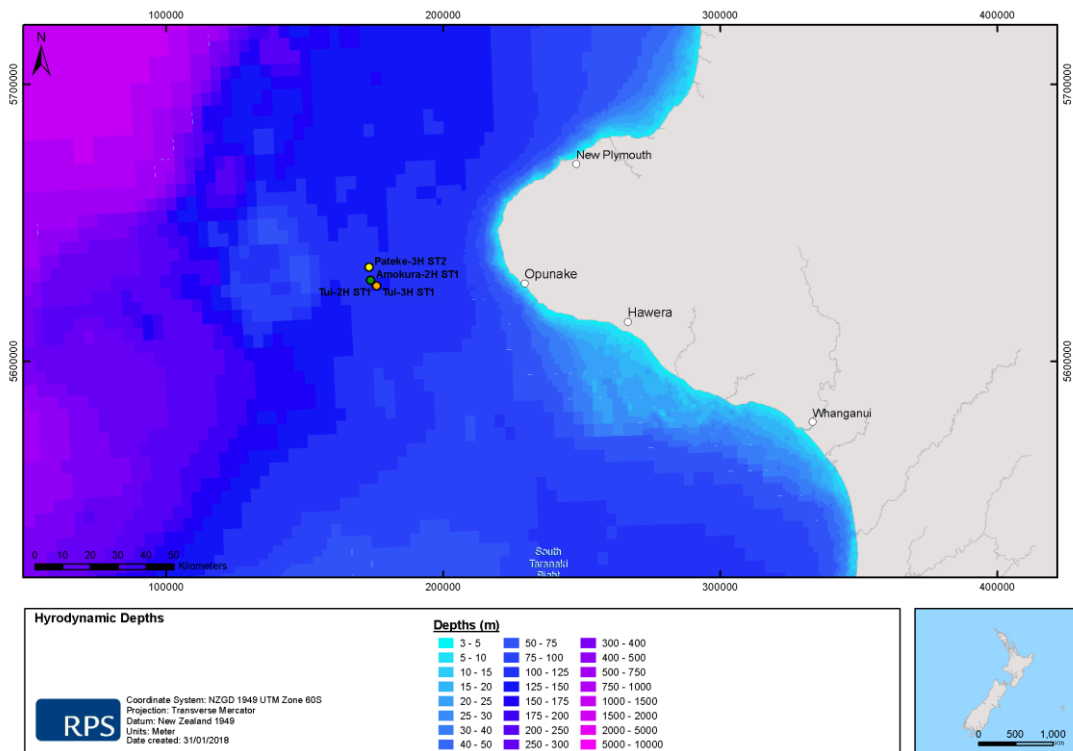


Figure 4 Bathymetry used in the hydrodynamic grid for the study region.

3.1.2 Tidal Conditions

The ocean boundary data for the regional model was obtained from satellite measured altimetry data (TOPEX/Poseidon 7.2) which provided estimates of the eight dominant tidal constituents at a horizontal scale of approximately 0.25 degrees. The eight major tidal constituents used were K_2 , S_2 , M_2 , N_2 , K_1 , P_1 , O_1 and Q_1 . Using the tidal data, surface heights were firstly calculated along the open boundaries, at each time step in the model.

The Topex-Poseidon satellite data is produced, and quality controlled by National Aeronautics and Space Administration (NASA). The satellites, equipped with two highly accurate altimeters, capable of taking sea level measurements accurate to less than ± 5 cm, measured oceanic surface elevations (and the resultant tides) for over 13 years (1992–2005). In total these satellites carried out 62,000 orbits of the planet. The Topex-Poseidon tidal data has been widely used amongst the oceanographic community, being the subject of more than 2,100 research publications (e.g. Andersen, 1995; Ludicone et al., 1998; Matsumoto et al., 2000; Kostianoy et al., 2003; Yaremchuk and Tangdong, 2004; Qiu and Chen 2010). As such the Topex/Poseidon tidal data is considered suitably accurate for this study.

3.1.3 Surface Elevation Validation

To ensure that tidal predictions were accurate, predicted surface elevations were compared to data observed at five locations situated across the study region (Figure 5).

Figure 6 to Figure 8 illustrate a comparison of the predicted and observed surface elevations for each location for January 2014. As shown on the graph, the model accurately reproduced the phase and amplitudes throughout the spring and neap tidal cycles.

To provide a statistical measure of the model's performance, the Index of Agreement (IOA – Willmott, 1981) and the Mean Absolute Error (MAE – Willmott, 1982; Willmott and Matsuura, 2005) were used.

The MAE is the average of the absolute values of the difference between the model-predicted (P) and observed (O) variables. It is a more natural measure of the average error and more readily understood (Willmott and Matsuura, 2005).

$$MAE = N^{-1} \sum_{i=1}^N |P_i - O_i|$$

The Index of Agreement (IOA) is determined by:

$$IOA = 1 - \frac{\sum |X_{model} - X_{obs}|^2}{\sum (|X_{model} - \bar{X}_{obs}| + |X_{obs} - \bar{X}_{obs}|)^2}$$

Where: X represents the variable being compared and the time mean of that variable. A perfect agreement exists between the model and field observations if the index gives an agreement value of 1 and complete disagreement will produce an index measure of 0 (Willmott, 1981). Willmott et al., (1985) also suggests that values meaningfully larger than 0.5 represent good model performance. Clearly, a greater IOA and lower MAE represent a better model performance.

Table 2 shows the IOA and MAE values for the selected locations.

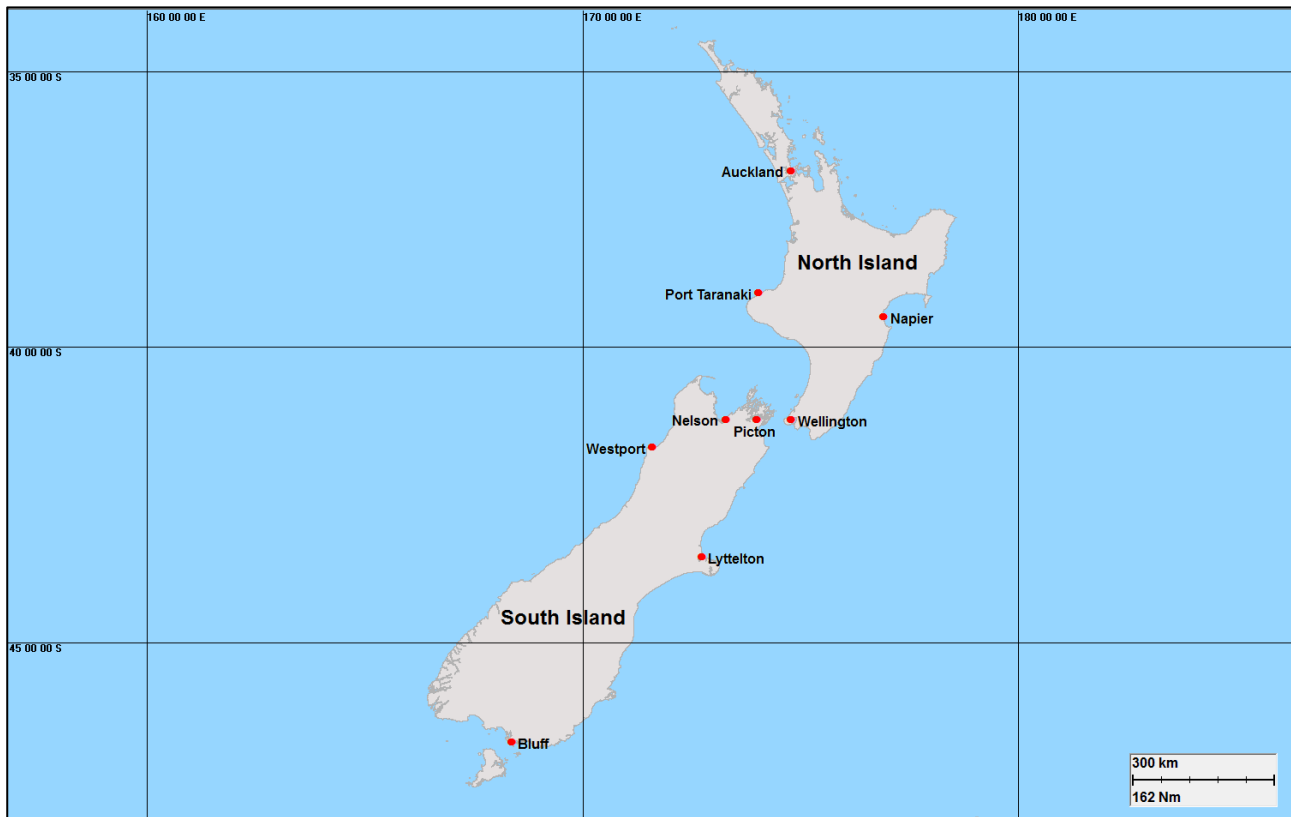


Figure 5 Location of the nine tide stations around New Zealand used to validate the tidal model.

Table 2 Statistical comparison between the observed and HYDROMAP predicted surface elevations data from the 1st to 31st January 2014.

Tide Station	IOA	MAE (m)
Auckland (North Island)	0.95	0.29
Bluff (South Island)	0.93	0.25
Lyttelton (South Island)	0.91	0.26
Napier (North Island)	0.98	0.11
Nelson (South Island)	0.93	0.39
Picton (South Island)	0.93	0.15
Port Taranaki (North Island)	0.94	0.33
Wellington (North Island)	0.95	0.13
Westport (South Island)	0.94	0.30
Average	0.94	0.25

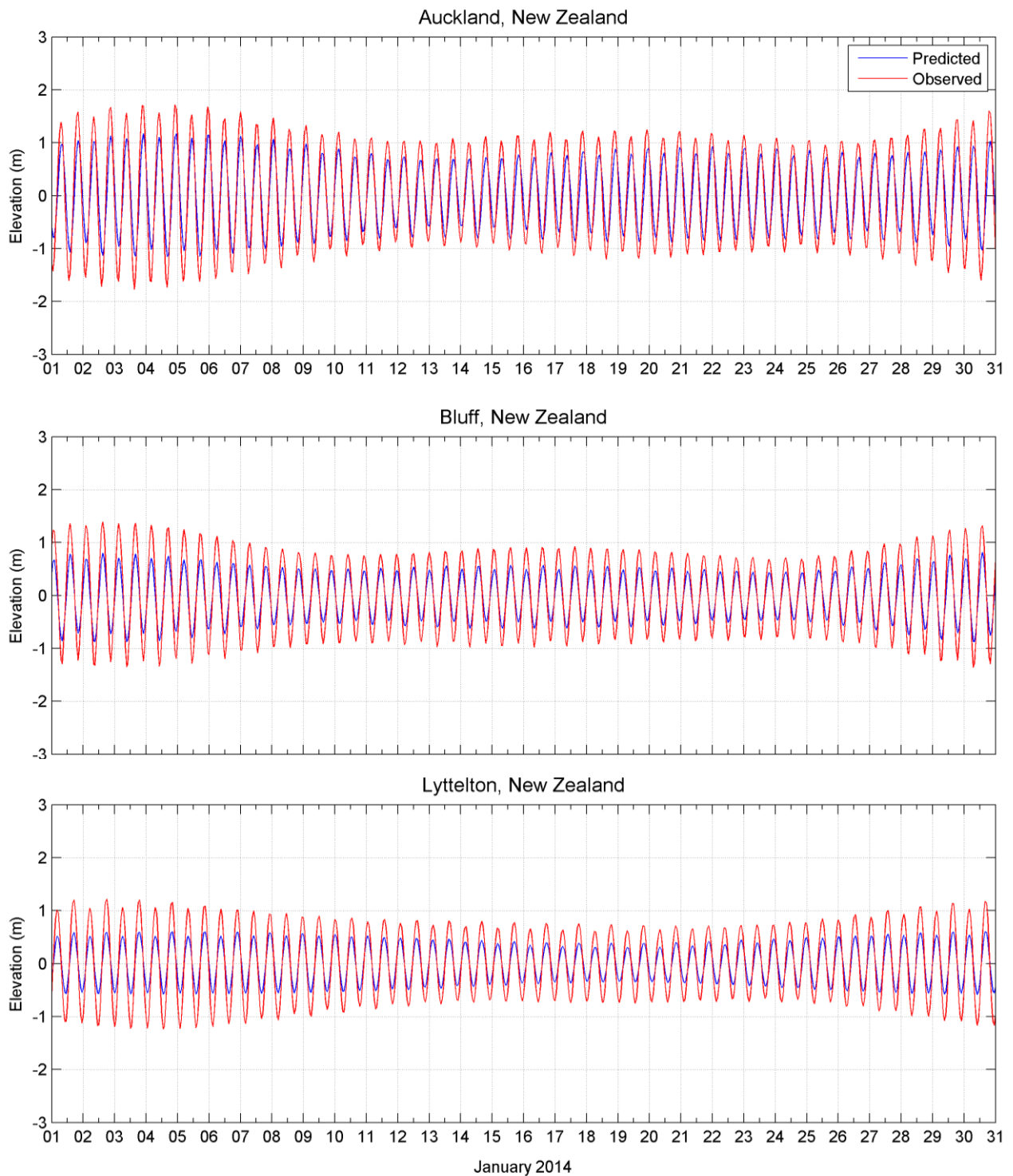


Figure 6 Comparison between predicted (red line) and observed (blue line) surface elevation variation at Auckland (top), Bluff (middle) and Lyttelton (bottom), between the 1st and the 31st of January 2014.

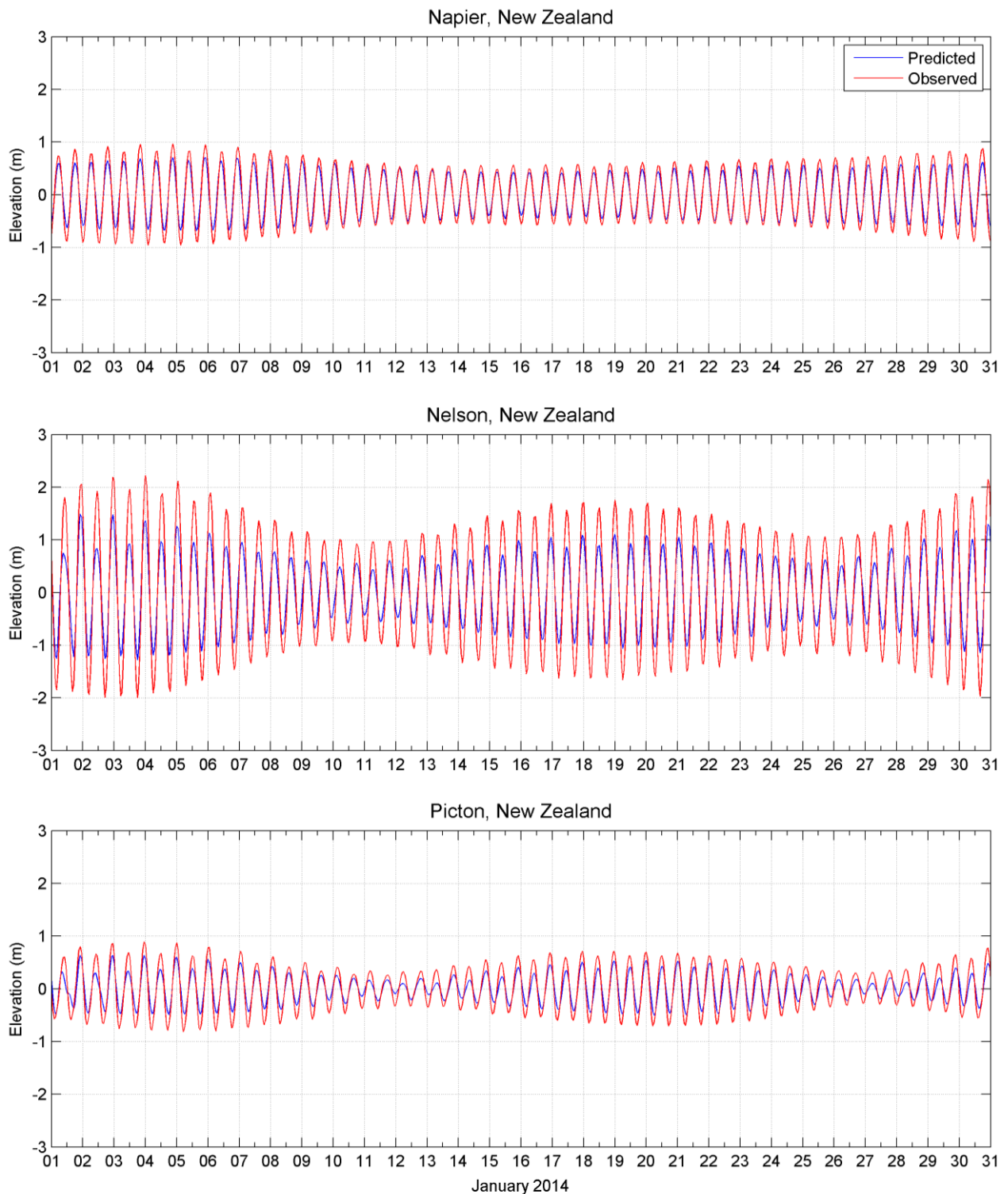


Figure 7 Comparison between predicted (red line) and observed (blue line) surface elevation variation at Napier (top), Nelson (middle) and Picton (bottom), between the 1st and the 31st of January 2014.

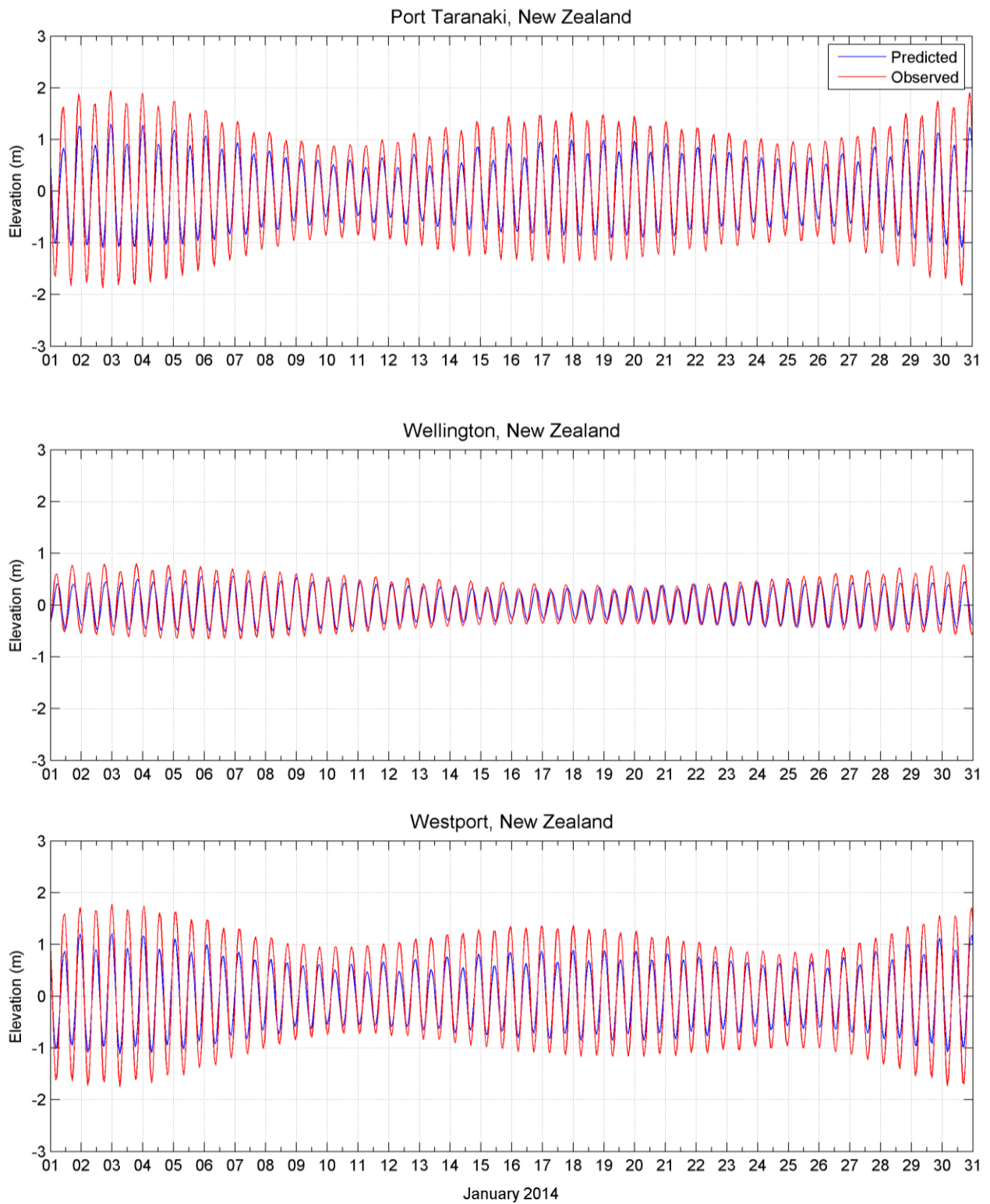


Figure 8 Comparison between predicted (red line) and observed (blue line) surface elevation variation at Port Taranaki (top), Wellington (middle) and Westport (bottom), between the 1st and 31st of January 2014.

3.2 Ocean Currents

Data describing the flow of ocean currents was obtained from HYCOM (Hybrid Coordinate Ocean Model, (Chassignet et al., 2007), which is operated by the HYCOM Consortium, sponsored by the Global Ocean Data Assimilation Experiment (GODAE). HYCOM is a data-assimilative, three-dimensional ocean model that is run as a hindcast (for a past period), assimilating time-varying observations of sea-surface height, sea-surface temperature and in-situ temperature and salinity measurements (Chassignet et al., 2009). The HYCOM predictions for drift currents are produced at a horizontal spatial resolution of approximately 8.25 km (1/12th of a degree) over the region, at a frequency of once per day. HYCOM uses isopycnal layers in the open, stratified ocean, but uses the layered continuity equation to make a dynamically smooth transition to a terrain-following coordinate in shallow coastal regions, and to z-level coordinates in the mixed layer and/or unstratified seas.

For this study, the HYCOM hindcast currents were obtained for the year 2012. Figure 9 shows an example of the modelled surface ocean currents (HYCOM) for the region.

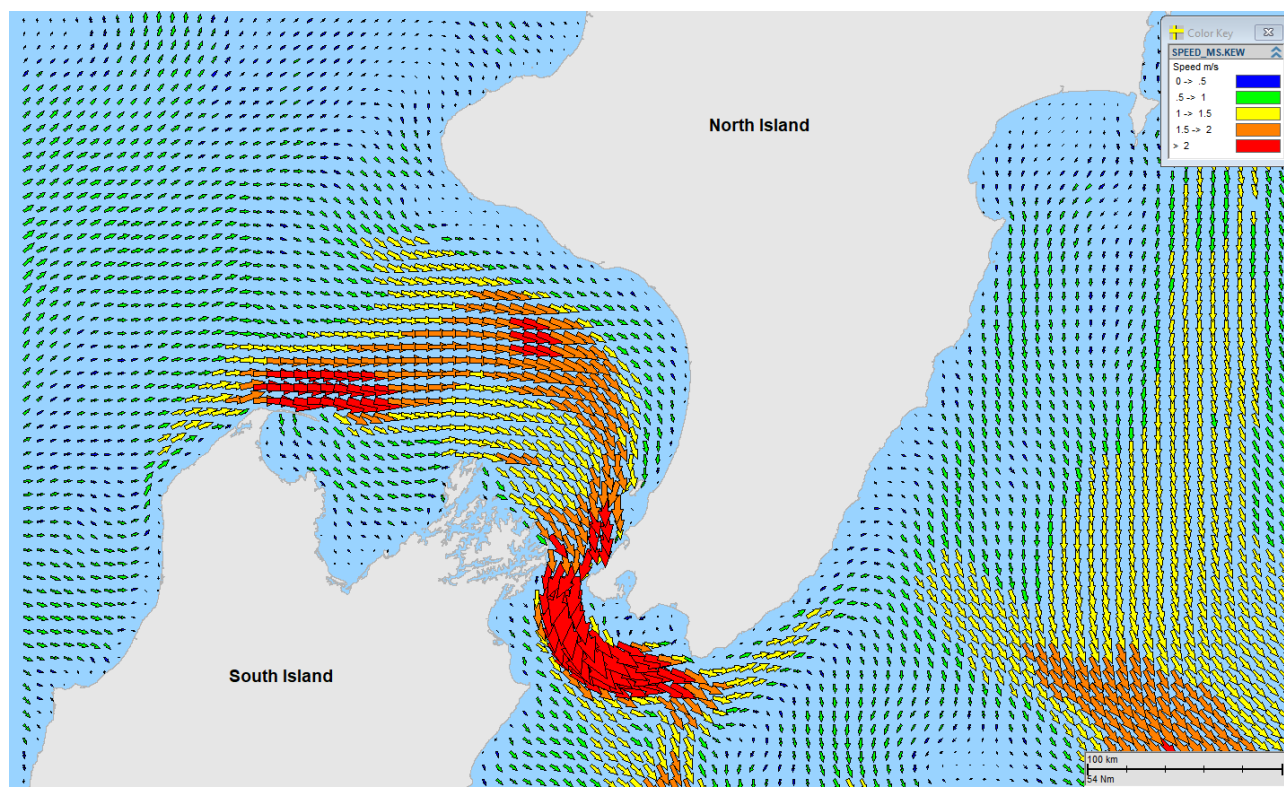


Figure 9 Snapshot example of the predicted HYCOM ocean surface currents in the region. Colour of individual arrows indicate current speed (m/s).

3.3 Currents at the Release Site

Table 3 displays the average and maximum combined surface current speeds (ocean plus tides) nearby the release sites. Figure 10 shows the monthly surface current rose distributions nearby the release sites.

Note the convention for defining current direction is the direction the current flows towards, which is used to reference current direction throughout this report. Each branch of the rose represents the currents flowing to that direction, with north to the top of the diagram. Sixteen directions are used. The branches are divided into segments of different colour, which represent the current speed ranges for each direction. Speed intervals of 0.1 m/s are typically used in these current roses. The length of each coloured segment is relative to the proportion of currents flowing within the corresponding speed and direction.

The data showed that the surface current speeds and directions were variable between the months, though with a predominant flow towards the south-southeast and north. The maximum and average surface current speeds were 1.44 m/s 0.24 m/s, respectively.

Table 3 Predicted average and maximum surface current speeds at the study site. The data was derived by combining the HYCOM ocean data and HYDROMAP tidal data for 2008-2012 (inclusive).

Month	Average current speed (m/s)	Maximum current speed (m/s)	General Direction
January	0.24	1.17	Northeast to Southeast
February	0.20	0.96	Northeast to Southeast
March	0.23	1.37	Northwest and Southeast
April	0.25	1.44	Southeast
May	0.26	0.91	Southeast
June	0.25	1.04	Variable
July	0.24	1.10	Northwest to Northeast
August	0.23	1.21	South
September	0.27	1.32	Southeast
October	0.25	1.00	Northeast to southeast
November	0.23	1.07	Northeast
December	0.25	0.94	Southeast
Minimum	0.20	0.91	
Maximum	0.27	1.44	

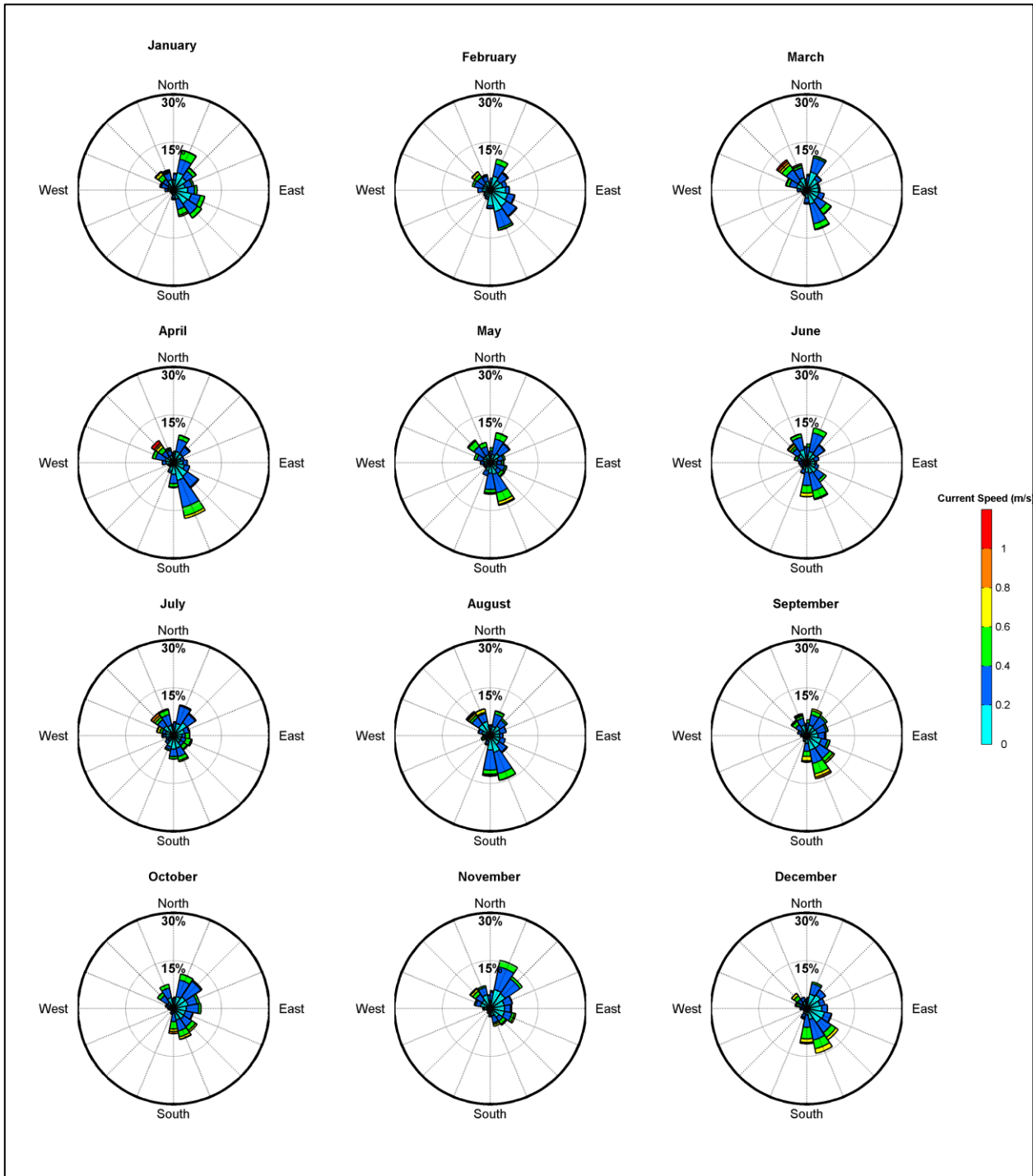


Figure 10 Predicted monthly surface current rose plots at the study site. Data was derived by combining the HYDROMAP tidal currents and HYCOM ocean currents for 2008 – 2012. The colour key shows the current speed (m/s), the compass direction provides the current direction flowing TOWARDS and the length of the wedge gives the percentage of the record for a particular speed and direction combination.

4 Water Temperature and Salinity

The monthly temperature and salinity profiles of the water column near the release site was obtained from the World Ocean Atlas 2013 database produced by the National Oceanographic Data Centre (National Oceanic and Atmospheric Administration) and its co-located World Data Center for Oceanography (see Levitus et al., 2013).

Monthly average sea-surface temperatures near the release site were found to vary over the course of the year from a minimum of 13.0°C (August) to a maximum of 19.1°C (March) (Table 4).

Monthly average salinity of the upper water column near the release site varied only slightly throughout the year from a minimum of 35.0 PSU (January and March) to a maximum of 35.3 PSU (July) (Table 4).

To accurately represent the sea temperature and salinity throughout the whole water column the modelling used monthly average sea temperature and salinity profiles, as presented in Figure 11.

Table 4 Monthly average sea-surface temperature and salinity at the study area.

Month	Jan	Feb	Mar	Apr	May	Jun	Jul	Aug	Sep	Oct	Nov	Dec
Temperature (°C)	17.8	19.1	19.1	17.6	16.2	14.9	14.4	13.0	13.6	13.9	14.9	16.1
Salinity (PSU)	35.0	35.1	35.0	35.2	35.2	35.2	35.3	35.2	35.1	35.1	35.1	35.2

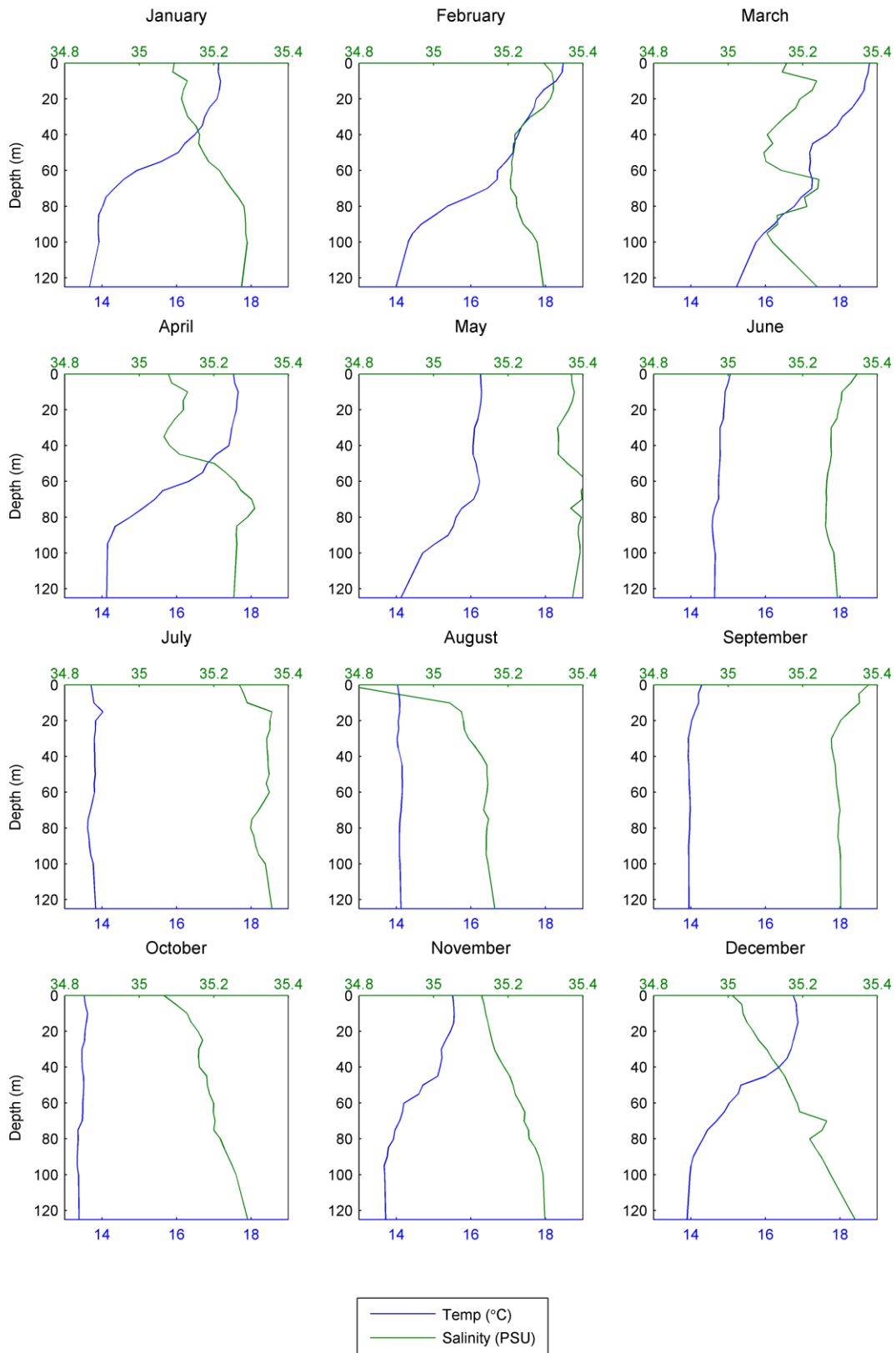


Figure 11 Monthly average sea temperature and salinity profiles at the study site.

5 Sediment Dispersion Modelling

5.1 Model Description - MUDMAP

MUDMAP is a three-dimensional plume model used by industry and regulators to aid in assessing the potential environmental effects from operational discharges such as drill cuttings, drilling fluids and produced water. The model has been applied to hundreds of assessments in over 35 countries, including New Zealand.

The model itself is an enhancement of the Offshore Operators Committee (OOC) model and calculates the fates of discharges through three distinct stages, as defined by laboratory and field studies (Koh and Chang 1973; Khondaker 2000):

- Stage 1: **Convective descent** – free fall of the combined mass of fluids and cuttings;
- Stage 2: **Dynamic collapse stage** – the collapse of the combined mass as it meets the seabed (or water surface);
- Stage 3: **Dispersion stage** – the transport and dispersion of discharged fluids and particles by the local currents. For cuttings and drilling mud particles that have higher density than seawater, this phase also calculates sinking and settlement to the seabed.

Each stage plays an integral role on different time and distance scales. The governing equations and solutions of MUDMAP were built on the formulas originally developed by Koh and Chang (1973) and are extended by the work of Brandsma and Sauer (1983), known as the OOC model, for Stages 1 and 2 of plume motion.

The far-field calculation (passive dispersion stage), employs a particle-based, random walk procedure. The model predicts the dynamics of the discharge material and resulting seabed concentrations and bottom thicknesses over the near-field (i.e. the immediate area of the discharge) and the far-field (the wider region). Figure 12 shows a conceptual diagram of the dispersion and fates of drill cuttings and fluids discharge to the ocean and an idealized representation of the three discharge phases.

Settling under currents is selective for particle size, with the larger particles (rock chips to sand) tending to settle quickly, forming a pile that aligns with the predominant current axis. Smaller particles (especially silts and clays) will remain suspended for longer periods and will therefore be dispersed more widely by the ambient current conditions. Dispersion of the finer discharged material will tend to be enhanced with increased current speeds and water depth and with greater variation in current direction over time and depth.

Along with the advanced analyses tools, MUDMAP can simulate six classes of material (with up to 36 sub-categories), each with unique density and particle-size distribution. During the dispersion stage, the model particles are transported in three-dimensions according to the current data and horizontal and vertical mixing coefficients at each time step according to the governing equations.

MUDMAP has been extensively validated and applied for discharge operations in Australian coastal waters (e.g. Burns et. al. 1999; King and McAllister 1997, 1998; Spaulding, 1994).

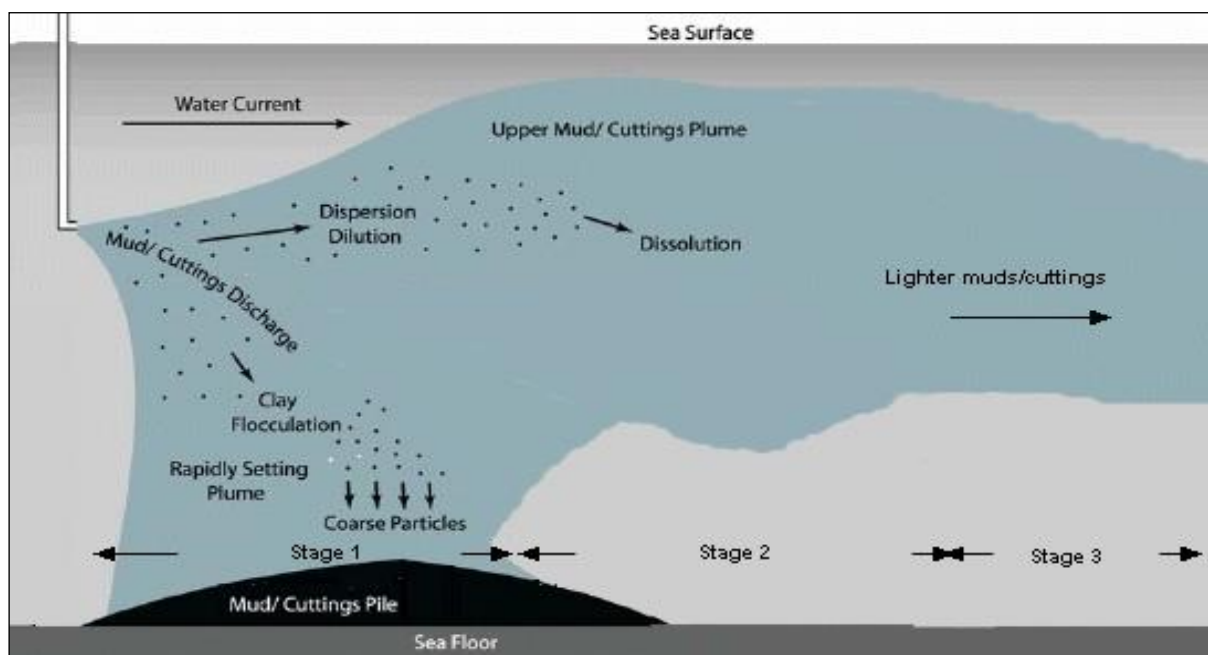


Figure 12 Conceptual diagram showing the general behaviour of cuttings and muds following discharge to the ocean (Neff, 2005) and the idealised representation of the three discharge phases.

5.2 Discharge Program

Tamarind has indicated that the wells will reuse existing conductor holes, so these new sections will consist of only 8½" production holes (Table 5). Drilling will commence first at Amokura-2H, then Tui-2H and 3H, followed by Pateke-3H and drilling durations for each well varied from 11.8 days to 17.8 days. All sections will be using water-based muds and a riser would be fitted to circulate cuttings and drilling fluid to the drilling rig where the cuttings and muds would be separated before the cuttings and unrecoverable mud solids are discharged at a depth of 10 m below the sea surface from a vertically downward orientated discharge pipe. Estimates for the volumes of mud solids discharged during this drilling are based on assumed rates of loss from the separation system, adhering to the cuttings.

Table 5 Summary of the estimated volume of discharged drill cuttings and unrecoverable mud solids for each well.

Well	Hole diameter (inches)	Discharge Method	Cuttings discharged (m ³)	Muds (solids only)		Discharge duration (days)
				Type	Volume discharged (m ³)	
Amokura-2H ST1	8½	10m below sea surface	108	WBM	27	15.4
Tui-2H ST1	8½	10m below sea surface	124.3	WBM	31.075	17.8
Tui-3H ST1	8½	10m below sea surface	82.6	WBM	20.65	11.8
Pateke-3H ST2	8½	10m below sea surface	112.2	WBM	28.05	16

Note: Only discharged solids used as model input.

WBM – Water Based Muds.

5.3 Discharge Input Data

The input data used to setup the dispersion model included:

- Volume and discharge duration of the cuttings and unrecovered muds;
- Particle size distributions and associated settling velocities of discharged cuttings and unrecoverable muds;
- Bulk density of the discharged cuttings and unrecoverable muds;
- Temperature and salinity profile of the receiving waters;
- The size and orientation of the discharge pipe;
- The height/depth of the discharge point relative to mean sea level; and
- Depth-varying current data to represent local physical forcing.

Table 6 provides a summary of the discharge configuration and the estimated volume of cuttings and muds used as input into the discharge model. Each simulation was run for an additional 7 days to allow finer sediments to settle out of suspension or to disperse.

A cuttings density of 2,400 kg/m³ and a mud density of 2,710 kg/m³ were used as model inputs. It is important to note that grain size has a greater influence on the rate of settling than density (Neff, 2005). The grain sizes are expected to vary between 0.016 mm and 6 mm in diameter. The fall velocities for the various size classes were derived from empirical data provided by Dyer (1986).

Table 7 shows the percentage contribution of each sediment size classes of the discharged material.

Table 6 Input data used for the drill cuttings and unrecoverable mud solids dispersion modelling.

Parameter/description	Amokura-2h	Tui-2H	Tui-3H	Pateke-3H
Volume of cuttings discharged near the sea surface (m ³)	108	124.3	82.6	112.2
Volume of muds discharged near the sea surface (m ³)	27	31.075	20.65	28.05
Bulk density of drill cuttings (kg/m ³)	2,400			
Bulk density of drilling water-base mud solids (kg/m ³)	2,710			
Discharge duration [model duration] (days)	15.4 [23]	17.8 [25]	11.8 [19]	16 [23]
Depth of sea surface discharges	10 m below mean sea level			
Sea surface discharge pipe orientation	Vertically downwards			
Sea surface discharge pipe diameter	16"			
Model conditions	Calendar month of January (2012)	Calendar month of February (2012)	Calendar month of April (2012)	Calendar month of May (2012)

Table 7 Discharged grain size distribution and settling velocities assumed for the production wells consisting of cuttings and water-based mud.

Class	Grain size (mm)	Settling velocity (cm/s)	Well section consisting of cuttings and WBM (composition %)
Large cuttings	6	53.62	9.57
	5	49.46	9.57
	2	28.55	9.57
	1	12.73	6.45
	0.5	7.5	6.45
	0.45	6.6	3.23
Medium cuttings	0.4	6	3.23
	0.35	5	3.12
	0.3	4	3.12
	0.25	3.1	3.12
	0.2	2.3	3.12
	0.15	1.6	3.12
Light cuttings	0.1	0.8	3.12
	0.05	0.22	3.12
	0.04	0.15	3.23
	0.03	0.08	3.23
	0.02	0.04	3.23
Drilling mud solids	0.063	0.34	0.45
	0.05	0.22	1.14
	0.035	0.11	2.63
	0.026	0.06	4.27
	0.02	0.038	5.27
	0.016	0.026	6.69

5.4 Grid Configuration

A grid covering a 20 km (longitude, x-direction) by 20 km (latitude, y-direction) region with each grid cell being 20 m (x) x 20 m (y) was employed to calculate the thickness of deposited drill cuttings and muds on the seafloor, with vertical divisions of 10 m to allow for assessing total suspended solids in the water column.

5.5 Mixing Parameters

A horizontal coefficient value of 0.1 m²/s and a vertical coefficient value of 0.01 m²/s was applied to account for turbulent mixing processes that occur as the discharged material disperses from the near-surface release point.

5.6 Minimum Reporting Thresholds

As the MUDMAP model has the ability to track cuttings and muds to thicknesses (and concentrations) that are lower than biologically significant, it was necessary to specify a minimum reporting threshold for the predicted bottom thickness which would record the “exposure” on the seafloor above natural sedimentation rates.

The threshold adopted for sea floor deposition was calculated using a conservatively assumed background sedimentation rate of 10 g/m²/day. This sedimentation rate, multiplied by 40 days, which is the average time to complete each well, provides a deposition threshold of 400 g/m². This deposition threshold was converted to a minimum thickness by considering the average bulk density of the cuttings and mud solids. To account for voids within the newly settled cuttings and muds a bulking factor of 2.5 was applied to give a final minimum deposition thickness threshold of 0.4 mm (or 400 µm). This same bulking factor was applied to the modelling results.

Total suspended solids (TSS) thresholds were set to a conservative level of 1 mg/l.

6 Results

Table 8 to Table 11 provide a summary of deposition on the sea floor for each well, above the minimum threshold of 0.4 mm (400 μm), while Figure 13 to Figure 15 show the spatial distributions of the sea floor deposition.

Maximum thickness on the sea floor ranged from 86 mm for the Pateke-3H well to 105 mm for the combined Tui wells. These maximum thicknesses occurred within 20 meters of the well.

Sea floor deposition greater than the 0.4 mm threshold reached maximum distances ranging from 204 m for the Amokura-2H well to 306 m for the combined Tui wells.

The maximum areas of sea floor coverage above the minimum threshold of 0.4 mm ranged from 84,930 m^2 (0.085 km^2) for the Amokura-2H well to 194,600 m^2 (0.195 km^2) for the combined Tui wells.

Table 12 to Table 15 provide a summary of peak TSS concentrations in the water column for each well, above the minimum threshold of 1 mg/l, while Figure 16 to Figure 18 show the spatial distributions of the in-water TSS along with a cross-section to demonstrate the depth of penetration..

Peak TSS values at the well sites were consistent, with a maximum of 33 mg/l.

Maximum peak TSS values greater than the 1 mg/l threshold reached maximum distances ranging from 500 m for the Amokura-2H well to 571 m for the Pateke-3H well.

The total areas of influence by TSS values greater than the threshold of 1 mg/l ranged from 282,390 m^2 (0.282 km^2) for the Amokura-2H well to 604,000 m^2 (0.604 km^2) for the combined Tui wells.

TSS concentrations of 10 mg/l were only observed in the top 20 m of the water column, while TSS concentrations down to 2 mg/l were only observed down to 30 or 40 m.

TSS concentrations greater than 1 mg/l extended almost all the way to the seabed directly under the discharge site, due to material falling through this column of water, however further afield TSS concentrations greater than 1 mg/l were only observed in the top 30 to 40 m of the water column.

Table 8 Predicted bottom deposition, area of coverage and maximum distance to the minimum threshold for each well.

Well	Maximum bottom thickness (mm)	Total area of coverage above 0.4 mm minimum threshold (km ²)	Maximum distance from the well to the 0.4 mm minimum threshold (m)
Amokura-2H	97	0.085	204
Tui-2H and 3H Combined	105	0.195	306
Pateke-3H	86	0.097	217

Table 9 Total area covered for each bottom deposition range for Amokura-2H.

Thickness Range (mm)	Cumulative area of coverage (m ²)	Maximum distance from well (m)
>0.4	84,930	204
>0.8	44,280	149
>1.6	27,380	117
>3.2	15,660	90
>6.5	7,160	57

Table 10 Total area covered for each bottom deposition range for Tui-2H and 3H combined.

Thickness Range (mm)	Cumulative area of coverage (m ²)	Maximum distance from well (m)
>0.4	194,600	306
>0.8	86,100	214
>1.6	44,800	164
>3.2	29,000	130
>6.5	14,800	90

Table 11 Total area covered for each bottom deposition range for Pateke-3H.

Thickness Range (mm)	Cumulative area of coverage (m ²)	Maximum distance from well (m)
>0.4	96,760	217
>0.8	51,540	155
>1.6	30,900	125
>3.2	16,800	92
>6.5	7,160	56

Table 12 Predicted total suspended solids concentration for each well

Well	Maximum peak total suspended solids concentration (mg/l)	Total area of coverage above 1 mg/l minimum threshold (km ²)	Maximum distance from the well to the 1 mg/l minimum threshold (m)
Amokura-2H	33	0.282	500
Tui-2H and 3H Combined	32	0.604	541
Pateke-3H	32	0.308	571

Table 13 Total area covered for each total suspended solids concentration range for Amokura-2H.

TSS Concentration (mg/l)	Cumulative area of coverage (m ²)	Maximum distance from well (m)
>1	282,390	500
>2	50,500	183
>5	4,150	45
>10	1,660	28
>20	310	17

Table 14 Total area covered for each total suspended solids concentration range for Tui-2H and 3H combined.

TSS Concentration (mg/l)	Cumulative area of coverage (m ²)	Maximum distance from well (m)
>1	604,000	541
>2	95,900	150
>5	8,300	46
>10	3,300	31
>20	900	19

Table 15 Total area covered for each total suspended solids concentration range for Pateke-3H.

TSS Concentration (mg/l)	Cumulative area of coverage (m ²)	Maximum distance from well (m)
>1	307,800	571
>2	47,910	192
>5	4,770	52
>10	1,760	29
>20	410	19

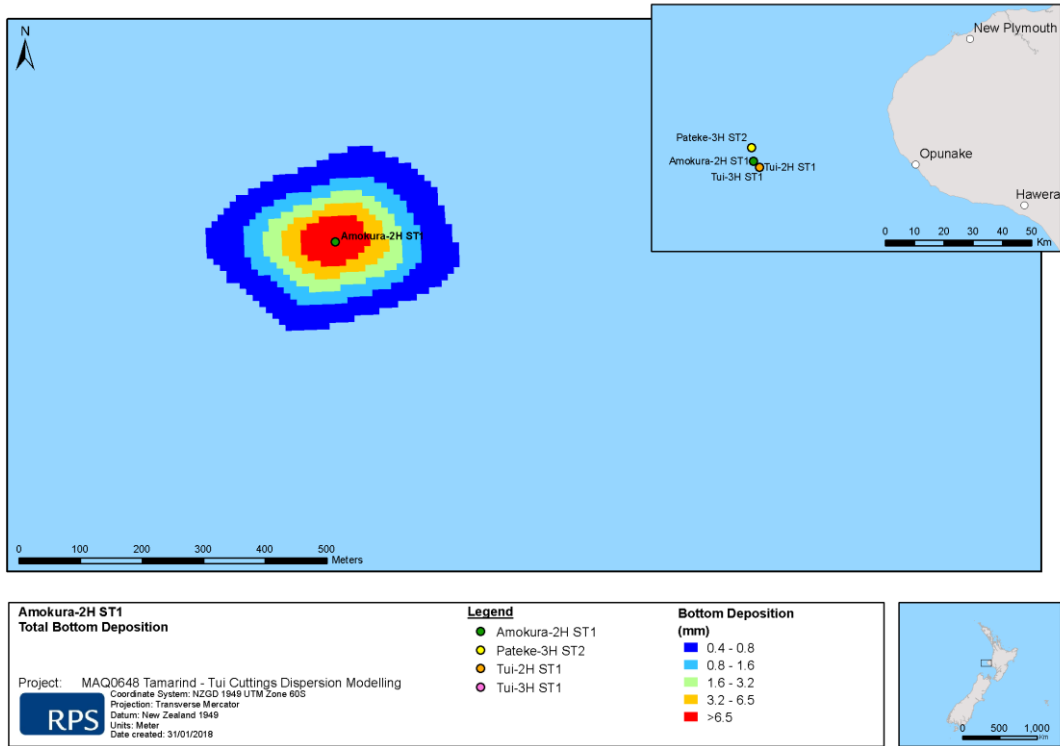


Figure 13 Predicted bottom deposition and coverage from drill cuttings and unrecoverable mud solids on the seafloor for Amokura-2H.

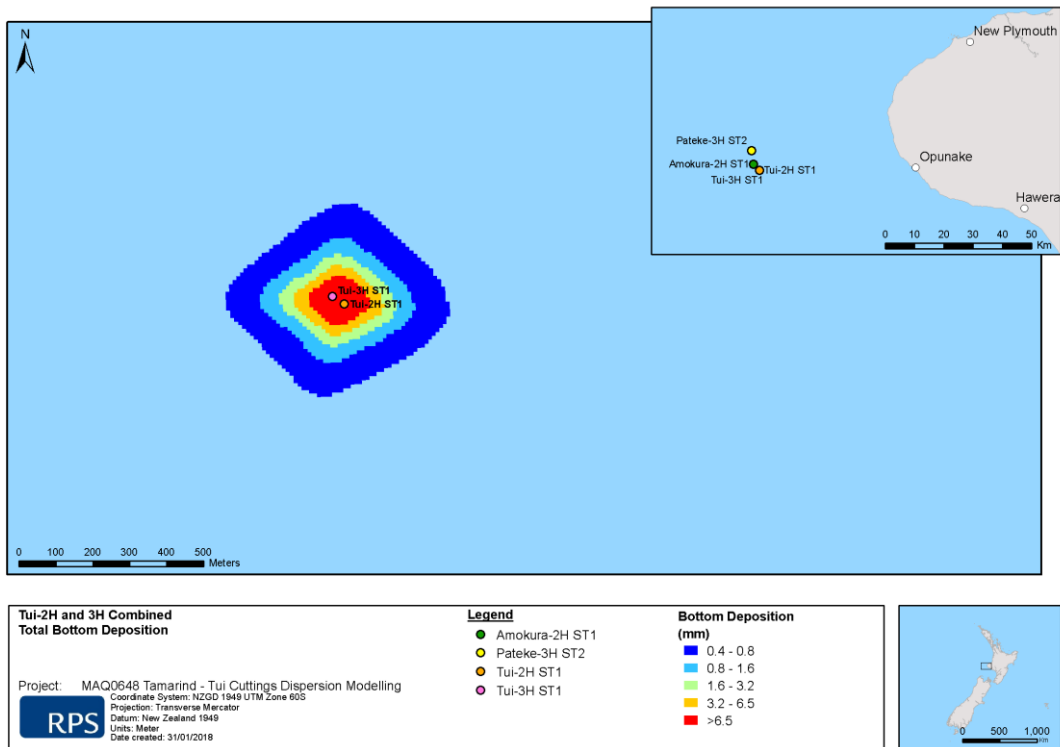


Figure 14 Predicted bottom deposition and coverage from drill cuttings and unrecoverable mud solids on the seafloor for Tui-2H and 3H combined.

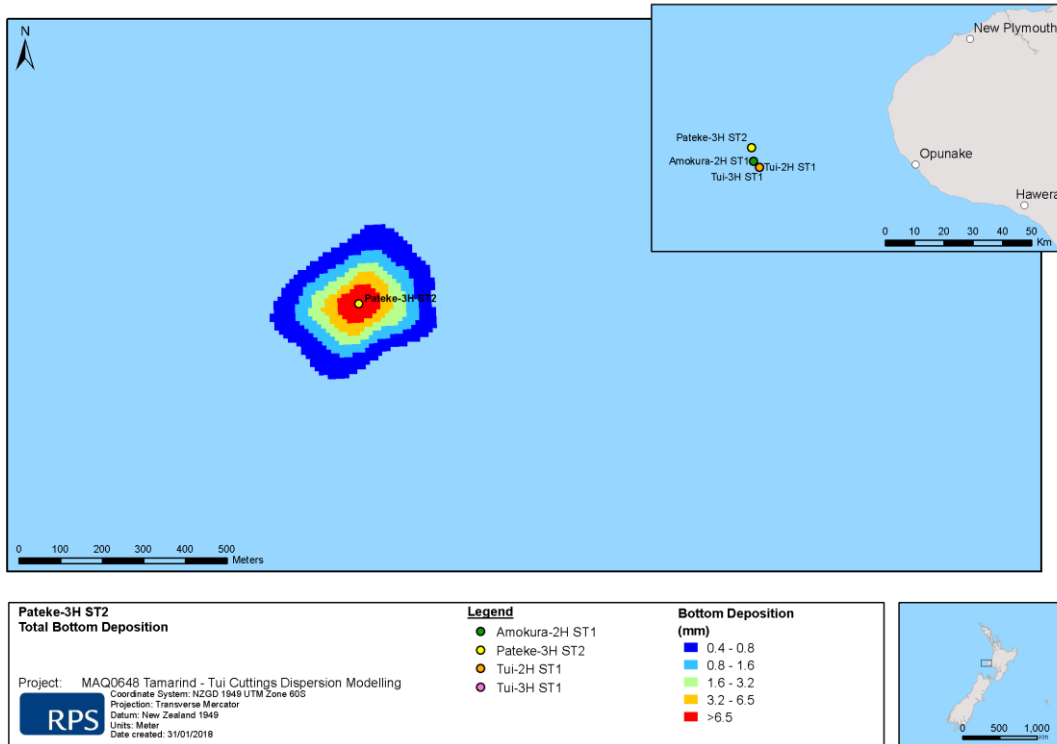


Figure 15 Predicted bottom deposition and coverage from drill cuttings and unrecoverable mud solids on the seafloor for Pateke-3H.

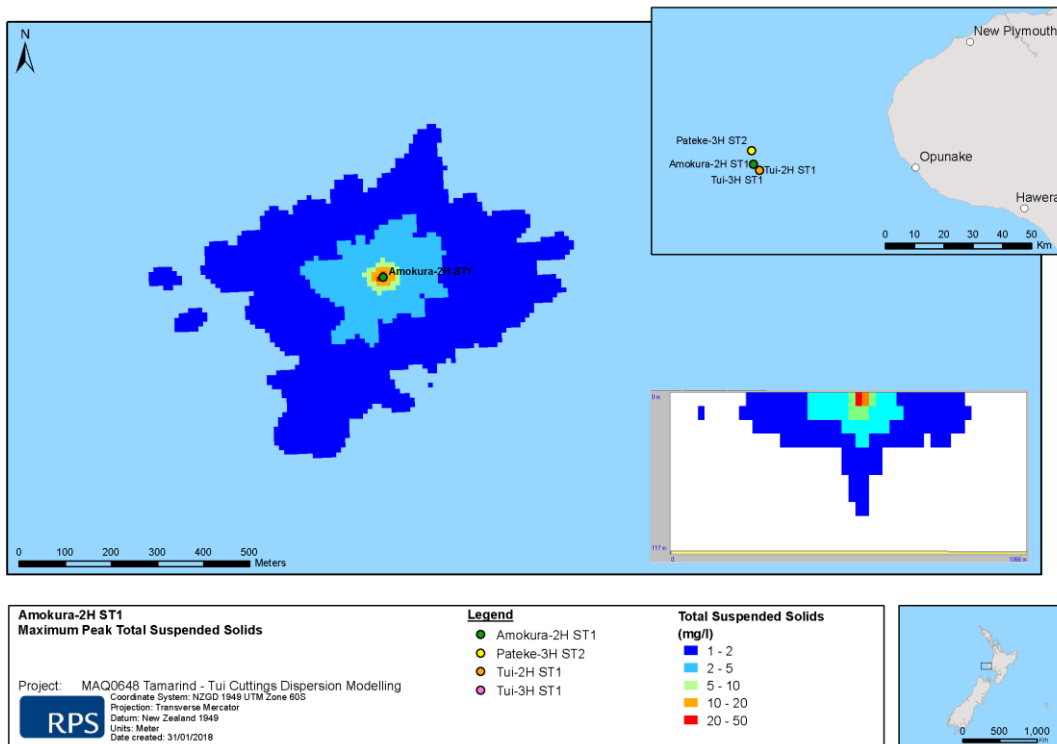


Figure 16 Predicted peak total suspended solids from drill cuttings and unrecoverable mud solids in the water column for Amokura-2H.

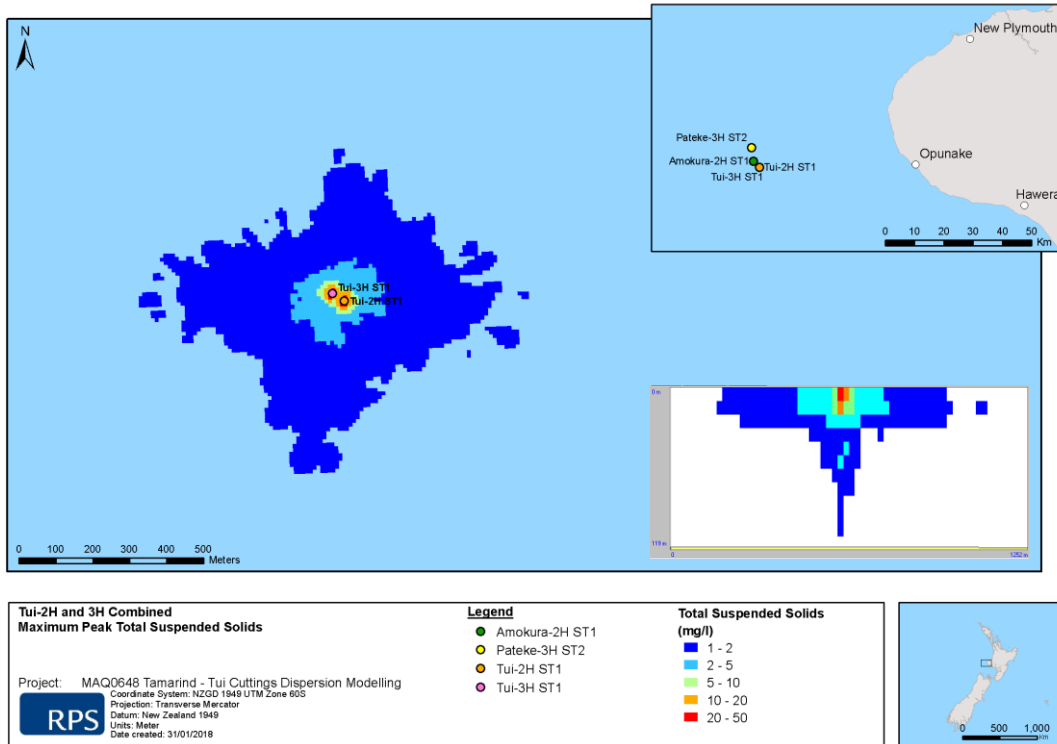


Figure 17 Predicted peak total suspended solids from drill cuttings and unrecoverable mud solids in the water column for Tui-2H and 3H combined.

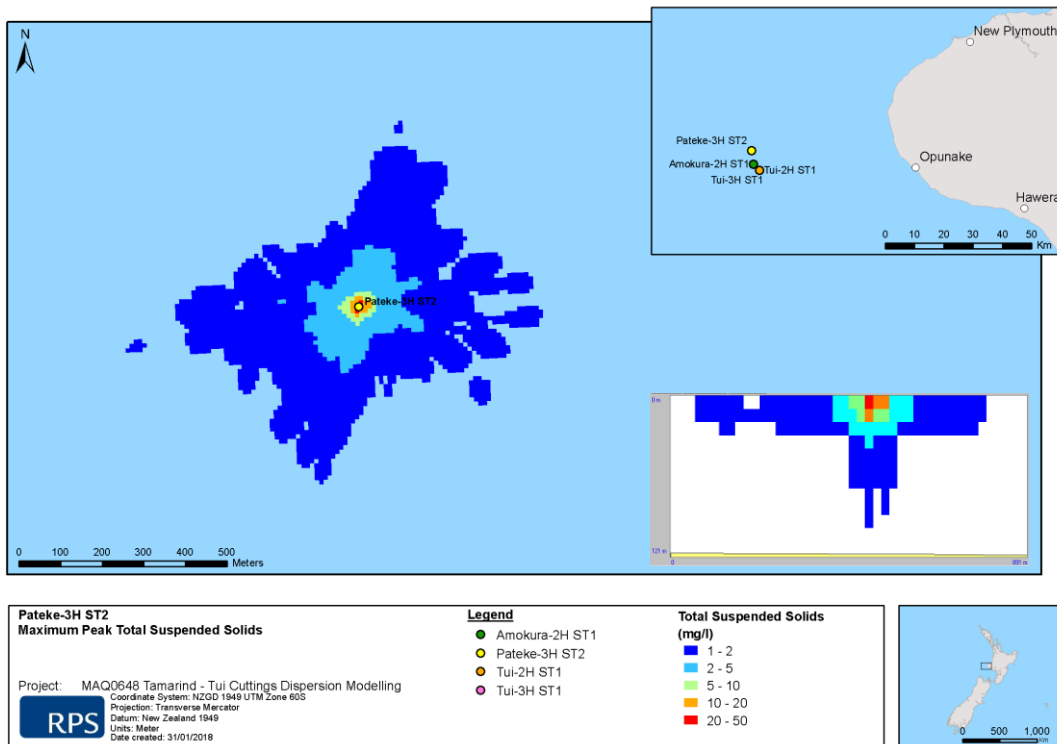


Figure 18 Predicted peak total suspended solids from drill cuttings and unrecoverable mud solids in the water column for Pateke-3H.

7 References

- Andersen, OB 1995, 'Global ocean tides from ERS 1 and TOPEX/POSEIDON altimetry', *Journal of Geophysical Research: Oceans*, vol. 100, no. C12, pp. 25249–25259.
- Becker, JJ, Sandwell, DT, Smith, WHF, Braud, J, Binder, B, Depner, J, Fabre, D, Factor, J, Ingalls, S, Kim, S-H, Ladner, R, Marks, K, Nelson, S, Pharaoh, A, Trimmer, R, Von Rosenberg, J, Wallace, G & Weatherall, P 2009, 'Global bathymetry and evaluation data at 30 arc seconds resolution: SRTM30_PLUS', *Marine Geodesy*, vol. 32, no. 4, pp. 355–371.
- Bowman, MJ, Kibblewhite, AC, Murtagh, RA, Chiswell, SM & Sandersin, BG 1983, 'Circulation and mixing in greater Cook Strait, New Zealand', *Oceanologica Acta*, vol. 6, no. 4, pp. 383–391.
- Brandsma, MG & Sauer Jr, TC 1983. 'The OOC model: prediction of short term fate of drilling mud in the ocean, Part I model description and Part II model results', *Proceedings of Workshop on An Evaluation of Effluent Dispersion and Fate Models for OCS Platforms*, Minerals Management Service, Santa Barbara, pp. 86–106.
- Brodie, JW 1960, 'Coastal surface currents around New Zealand', *New Zealand Journal of Geology and Geophysics*, vol. 3, no. 2, pp. 235–252.
- Burns, K, Codi, S, Furnas, M, Heggie, D, Holdway, D, King, B, & McAllister, F 1999, 'Dispersion and Fate of Produced Formation Water Constituents in an Australian Northwest Shelf Shallow Water Ecosystem', *Marine Pollution Bulletin*, vol. 38, no. 7, pp. 593–603.
- Chassignet, EP, Hurlburt, HE, Smedstad, OM, Halliwell, GR, Hogan, PJ, Wallcraft, AJ, Baraille, R & Bleck, R 2007, 'The HYCOM (hybrid coordinate ocean model) data assimilative system', *Journal of Marine Systems*, vol. 65, no. 1, pp. 60–83.
- Chassignet, E, Hurlburt, H, Metzger, E, Smedstad, O, Cummings, J & Halliwell, G 2009, 'U.S. GODAE: Global Ocean Prediction with the HYbrid Coordinate Ocean Model (HYCOM)', *Oceanography*, vol. 22, no. 2, pp. 64–75.
- Coleman, R 1984, 'Investigation of the Tasman Sea by satellite altimetry', *Australian Journal of Marine and Freshwater Research*, vol. 35, no. 6, pp. 619–633.
- Davies, AM 1977a, 'The numerical solutions of the three-dimensional hydrodynamic equations using a B-spline representation of the vertical current profile', in JC Nihoul (ed), *Bottom Turbulence: Proceedings of the 8th Liège Colloquium on Ocean Hydrodynamics*, Elsevier Scientific, Amsterdam, pp. 1–25.
- Davies, AM 1977b, 'Three-dimensional model with depth-varying eddy viscosity', in JC Nihoul (ed), *Bottom Turbulence: Proceedings of the 8th Liège Colloquium on Ocean Hydrodynamics*, Elsevier Scientific, Amsterdam, pp. 27–48.
- Dyer, KR 1986, *Coastal and Estuarine Sediment Dynamics*, John Wiley & Sons Ltd., Chichester.
- Gordon, R 1982, Wind driven circulation in Narragansett Bay, Doctor of philosophy thesis, University of Rhode Island, Kingston.

- Heath, RA 1985, 'Large-scale influence of the New Zealand seafloor topography on western boundary currents of the South Pacific Ocean', *Australian Journal of Marine and Freshwater Research*, vol. 36, no. 1, pp. 1–14.
- Isaji, T & Spaulding, M 1984, 'A model of the tidally induced residual circulation in the Gulf of Maine and Georges Bank', *Journal of Physical Oceanography*, vol. 14, no. 6, pp. 1119–1126.
- Isaji, T, Howlett, E, Dalton C, & Anderson, E 2001, 'Stepwise-continuous-variable-rectangular grid hydrodynamics model', *Proceedings of the 24th Arctic and Marine Oil spill Program (AMOP) Technical Seminar (including 18th TSOCS and 3rd PHYTO)*, Environment Canada, Edmonton, pp. 597–610.
- Khondaker, AN 2000, 'Modeling the fate of drilling waste in marine environment – an overview', *Journal of Computers and Geosciences*, vol. 26, no. 5, pp. 531–540.
- King, B & McAllister, FA 1997, *Modelling the Dispersion of Produced Water Discharge in Australia 1 & 2*. Australian Institute of Marine Science, Townsville.
- King, B & McAllister, FA 1998, 'Modelling the dispersion of produced water discharges', *APPEA Journal*, pp. 681–691.
- Koh, RCY & Chang, YC 1973. *Mathematical model for barged ocean disposal of waste*, U.S. Army Engineer Waterways Experiment Station, Vicksburg.
- Kostianoy, AG, Ginzburg, AI, Lebedev, SA, Frankignoulle, M & Delille, B 2003, 'Fronts and mesoscale variability in the southern Indian Ocean as inferred from the TOPEX/POSEIDON and ERS-2 Altimetry data', *Oceanology*, vol. 43, no. 5, pp. 632–642.
- Levitus, S, Antonov, JI, Baranova, OK, Boyer, TP, Coleman, CL, Garcia, HE, Grodsky, AI, Johnson, DR, Locarnini, RA, Mishonov, AV, Reagan, JR, Sazama, CL, Seidov, D, Smolyar, I, Yarosh, ES & Zweng, MM 2013, 'The World Ocean Database', *Data Science Journal*, vol. 12, no. 0, pp. WDS229–WDS234.
- Ludicone, D, Santoleri, R, Marullo, S & Gerosa, P 1998, 'Sea level variability and surface eddy statistics in the Mediterranean Sea from TOPEX/POSEIDON data', *Journal of Geophysical Research I*, vol. 103, no. C2, pp. 2995–3011.
- Matsumoto, K, Takanezawa, T & Ooe, M 2000, 'Ocean tide models developed by assimilating TOPEX/POSEIDON altimeter data into hydrodynamical model: A global model and a regional model around Japan', *Journal of Oceanography*, vol. 56, no.5, pp. 567–581.
- Neff, J 2005, *Composition, environment fates, and biological effect of water based drilling fluids and cuttings discharged to the marine environment: A synthesis and annotated bibliography*, Battelle, Duxbury.
- Owen, A., 1980, 'A three-dimensional model of the Bristol Channel', *Journal of Physical Oceanography*, vol. 10, no. 8, pp. 1290–1302.
- Qiu, B & Chen, S 2010, 'Eddy-mean flow interaction in the decadal modulating Kuroshio Extension system', *Deep-Sea Research II*, vol. 57, no. 13, 1098–1110.
- Spaulding, ML 1994, 'Drilling, production fluids dispersion predicted by model', *Offshore*, vol. 54, no. 4, pp. 78–82.

- Willmott, CJ 1981, 'On the validation of models', *Physical Geography*, vol. 2, no. 2, pp. 184–194.
- Willmott, CJ 1982, 'Some comments on the evaluation of model performance', *Bulletin of the American Meteorological Society*, vol. 63, no. 11, pp. 1309–1313.
- Willmott CJ, Ackleson SG, Davis RE, Feddema JJ, Klink, KM, Legates, DR, O'Donnell, J & Rowe, CM 1985, 'Statistics for the evaluation of model performance', *Journal of Geophysical Research*, vol. 190, no. C5, pp. 8995–9005.
- Willmott, CJ & Matsuura, K 2005, 'Advantages of the mean absolute error (MAE) over the root mean square error (RMSE) in assessing average model performance', *Journal of Climate Research*, vol. 30, no. 1, pp. 79–82.
- Yaremchuk, M & Tangdong, Q 2004, 'Seasonal variability of the large-scale currents near the coast of the Philippines', *Journal of Physical Oceanography*, vol. 34, no. 4, pp. 844–855.
- Zigic, S, Zapata, M, Isaji, T, King, B, & Lemckert, C 2003, 'Modelling of Moreton Bay using an ocean/coastal circulation model', Proceedings of the 16th Australasian Coastal and Ocean Engineering Conference, the 9th Australasian Port and Harbour Conference and the Annual New Zealand Coastal Society Conference, Institution of Engineers Australia, Auckland, paper 170.